

Synthesis of Mesoporous Materials: Liquid-Crystal Templating versus Intercalation of Layered Silicates

J. C. Vartuli,^{*,†} C. T. Kresge,[‡] M. E. Leonowicz,[‡] A. S. Chu,[†] S. B. McCullen,[†]
I. D. Johnson,[‡] and E. W. Sheppard[†]

Mobil Research and Development Corporation, Central Research Laboratory,
Princeton, New Jersey 08543, and Paulsboro Research Laboratory,
Paulsboro, New Jersey 08066

Received May 10, 1994. Revised Manuscript Received August 4, 1994[®]

A comparison of the synthetic conditions required to form both MCM-41 and mesoporous materials obtained from layered silicates suggests that the mechanisms of formation of these two materials are different. X-ray diffraction patterns, transmission electron micrographs, sorption capacity measurements, and synthesis data are all consistent with MCM-41 formed by a silicate anion initiated liquid-crystal templating mechanism. Retention of the silicate layer throughout the synthetic process suggests that layered silicate derived materials are formed by the intercalation of the silicate layers. Although both materials are formed in the presence of a cationic surfactant, the surfactant functions in different roles. For MCM-41, the surfactant molecules form a micelle/liquid-crystal phase that serve as templates around which the silica condenses. The surfactant molecules in the layered silicate system function to swell and separate the layers. Rheological data of the surfactant solutions used in both synthesis systems also support the different formation mechanism pathways. At the surfactant concentrations typically used for MCM-41 formation, rheological data suggest the presence of micellar structure, whereas no solution structure was detected in the lower surfactant concentrations used in the layered silicate system. Although the intercalated silicate based materials can be synthesized with pores in a similar size range as MCM-41 products, the pore size distribution is broader. Also, MCM-41 materials have 5 times the total pore volume and hydrocarbon sorption capacity compared to the layered silicate derived materials.

Introduction

Two novel mesoporous materials have been recently reported.¹⁻³ Researchers at Mobil R&D Corp. introduced a new family of mesoporous molecular sieves, M41S, which exhibit narrow pore size distributions whose dimensions can be tailored from 15 to 100 Å.¹ The existence of several unique structures including MCM-41 (hexagonal) and MCM-48 (cubic) suggest that this family of mesoporous materials is extensive and versatile.² Yanagisawa et al.³ described a mesoporous silicate prepared from a layered silicate, kanemite. The latter material was prepared via a procedure similar to that used for the formation of MCM-41, namely, a hydrothermal synthesis in the presence of quaternary ammonium halides such as dodecyltrimethylammonium chloride or cetyltrimethylammonium chloride. The synthesis and swelling of kanemite was originally done by Lagaly,⁴ who demonstrated that this layered silicate could be intercalated by various quaternary ammonium

compounds and that the extent of interlayer separation was a function of the quaternary hydrocarbon chain length. Yanagisawa investigated this system and extended this work by calcining the quaternary-containing products. Not only did the resulting materials exhibit high surface area and pore volume but they also contain 30-40 Å size pores, similar to those properties associated with some of the members of MCM-41. Because of the similarities between the reported properties of this material and MCM-41, we investigated the characteristics of both of these mesoporous materials and propose different mechanistic pathways for their formation.

Experimental Section

Materials. The silica sources were sodium silicate, N brand, 27.8% silica, P.Q. Corp., and tetraethylorthosilicate (TEOS) obtained from Aldrich. Cetyltrimethylammonium chloride, C₁₆H₃₃(CH₃)₃NCl (CTMACl), was obtained from Ar-mak Chemicals as an aqueous solution (29 wt %). The dodecyltrimethylammonium bromide, C₁₂H₂₅(CH₃)₃NBr (DDT-MABr), was obtained from Aldrich. The C₁₆H₃₃(CH₃)₃N⁺OH/Cl⁻ solution was prepared by batch exchange of a 29 wt % aqueous CTMACl solution with IRA-400(OH) exchange resin, Rohm and Haas. The effective exchange of hydroxide for chloride ion was ~30%. Sulfuric acid (96.1%) and methanol (absolute) were obtained from J. T. Baker Chemical Co. All chemicals were used as received.

Instrumentation. X-ray powder diffraction was obtained on a Scintag XDS 2000 diffractometer using Cu K α radiation and an energy-dispersive detector. Benzene sorption data

[†] Mobil Research and Development Corp., Central Research Laboratory.

[‡] Mobil Research and Development Corp., Paulsboro Research Laboratory.

[®] Abstract published in *Advance ACS Abstracts*, October 1, 1994.

(1) Kresge, C. T.; Leonowicz, M. E.; Roth, W. J.; Vartuli, J. C.; Beck, J. S. *Nature*, **1992**, *359*, 710-712.

(2) Beck, J. S.; Vartuli, J. C.; Roth, W. J.; Leonowicz, M. E.; Kresge, C. T.; Schmitt, K. D.; Chu, C. T.-W.; Olson, D. H.; Sheppard, E. W.; McCullen, S. B.; Higgins, J. B.; Schlenker, J. L. *J. Am. Chem. Soc.* **1992**, *114*, 10834-43.

(3) Yanagisawa, T.; Shimizu, T.; Kiroda, K.; Kato, C. *Bull. Chem. Soc. Jpn.* **1990**, *63*, 988-992.

(4) Beneke, K.; Lagaly, G. *Am. Mineral.* **1977**, *62*, 763-771.

were obtained on a computer-controlled 990/951 DuPont TGA system. The calcined sample was dehydrated by heating at 350 or 500 °C to constant weight in flowing helium. Benzene sorption isotherms were measured at 25 °C by blending a benzene-saturated He gas stream with a pure helium gas stream in the proper proportions to obtain the desired benzene partial pressure. Argon physisorption measurements were conducted on a physisorption apparatus as previously described.⁵ The method of Horváth and Kawazoe⁶ was used to determine the pore diameters of the products. Rheological measurements of various surfactant solutions were obtained on a RFSII (Rheometrics Fluid Spectrometer II).

Samples for TEM examination were prepared using an ultramicrotome to obtain thin sections of the materials that had been embedded in L.R. White (hard) acrylic resin. Typical 500–1000 Å thick specimens were supported on 400 mesh copper electron microscope grids and lightly coated with evaporated carbon to reduce charging. Electron microscopy and electron diffraction experiments were done in a JEOL 200CX transmission electron microscope operated at 200 000 V. The microscope has an optimum interpretable resolution of 3.5 Å; an effective 2.8 Å objective aperture was employed to enhance image contrast.

Syntheses. A sample of kanemite was prepared by a method initially described by Lagaly⁴ and subsequently used by Yanagisawa et al.³ Sodium silicate solution (110 g) was added slowly with stirring to 500 g of methanol chilled in an ice bath. The product was recovered by filtration on a Buechner funnel, washed with water, and dried in air at ambient temperature. The dried material was then calcined in air at 700 °C for 5.5 h. The calcination procedure produced a low-density, highly porous product. This calcined material was then rehydrated in water, filtered, and allowed to dry in air at ambient temperature. This silicate product was used in the intercalation preparations described later. The X-ray diffraction pattern of the product was similar to that described in Table I of Lagaly.⁴ However, the relative peak intensities and the *d* spacings of the lower angle peaks in the X-ray diffraction pattern of our product differed from that material reported by Yanagisawa.³ The peak intensities and peak location of the X-ray diffraction patterns of layered silicates can be affected by both the degree of hydration and the extent of alkali content. Elemental analyses of our hydrated kanemite material contained a Na/Si/H₂O molar ratio of 0.4/2/2 compared to that of Lagaly⁴ (0.8/2/4) and that prepared by Yanagisawa³ (1/2/3).

The cetyltrimethylammonium (CTMA) intercalated kanemite was prepared as described by Yanagisawa³ by combining 100 g of a 0.1 M CTMACl solution and 1 g of the above-prepared kanemite with stirring at 65 °C for 1 week. The intercalated product was recovered by filtration and the above procedure was repeated with fresh 0.1 M CTMACl solution. The final product was recovered by filtration, dried in air at ambient temperature, and calcined in air to 540 °C for 6 h. The X-ray diffraction patterns of the 1- and 2-week intermediates and the calcined material are shown in Figure 1a, b, and c, respectively. Found in the 1-week as-synthesized product (wt %): C, 26.2; N, 1.27; Si, 24.9; ash (1000 °C), 59.4. Found in the final as-synthesized product (wt %): C, 25.7; N, 1.26; Si, 24.7; ash (1000 °C), 61.3.

The dodecyltrimethylammonium (DDTMA) intercalated kanemite was prepared by combining 100 g of a 0.1 M DDTMABr solution and 1 g of the hydrated kanemite with stirring at 65 °C for 1 week. The intercalated product was recovered by filtration, and the above procedure was repeated with fresh 0.1 M DDTMABr solution and processed to a calcined form using the method described above. The X-ray diffraction patterns of the 1- and 2-week intermediates and the calcined material are shown in Figure 2a, b, and c, respectively. Found in the 1-week as-synthesized product (wt

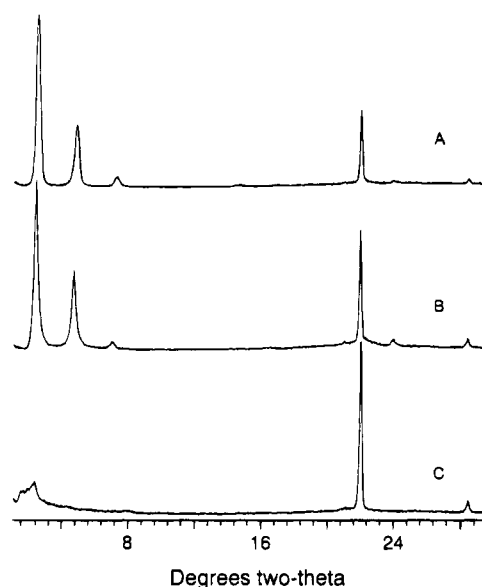


Figure 1. X-ray powder diffraction pattern of (A) CTMA-intercalated kanemite first week intermediate, (B) second week intermediate, and (C) calcined product.

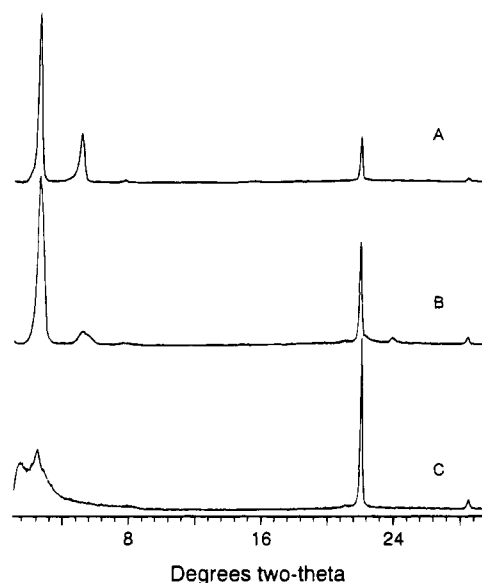


Figure 2. X-ray powder diffraction pattern of (A) DDTMA-intercalated kanemite first week intermediate, (B) second week intermediate, and (C) calcined product.

%) C, 20.6; N, 1.62; Si, 26.0; ash (1000 °C), 63.6. Found in the final as-synthesized product (wt %): C, 17.6; N, 1.06; Si, 26.9; ash (1000 °C), 69.1.

The hydrated kanemite was also combined with a 0.1 M C₁₆H₃₃(CH₃)₃N⁺ OH/Cl⁻ solution using the method described above. The first week sample produced an X-ray diffraction pattern having relatively intense peaks at *d* spacings of approximately 34, 17, 11, and 4 Å. After the second week of treatment, less than 10% of the original sample remained after filtration. This material exhibited an X-ray pattern with an intense peak at a *d* spacing of approximately 4 Å. No further processing was done on this sample.

Kenyaite,⁷ another layered silicate, was also subjected to the same procedure as described above. The X-ray diffraction patterns of the 1- and 2-week CTMA containing intermediates exhibited major peaks at *d* spacings of approximately 39 and 20 Å and a broad peak at approximately 3.4 Å. Upon calcination the CTMA intercalated kenyaite material exhibited an X-ray diffraction pattern containing major peaks at *d* spacings of 17, 8.5, and 3.4 Å similar to that of calcined kenyaite. There were no low-angle peaks remaining. If the

(5) Borghard, W. S.; Sheppard, E. W.; Schoennagel, H. J. *Rev. Sci. Instrum.* **1991**, *62*, 2801–2809.

(6) Horváth, G.; Kawazoe, K. *J. Chem. Eng. Jpn.* **1983**, *16*, 470–475.

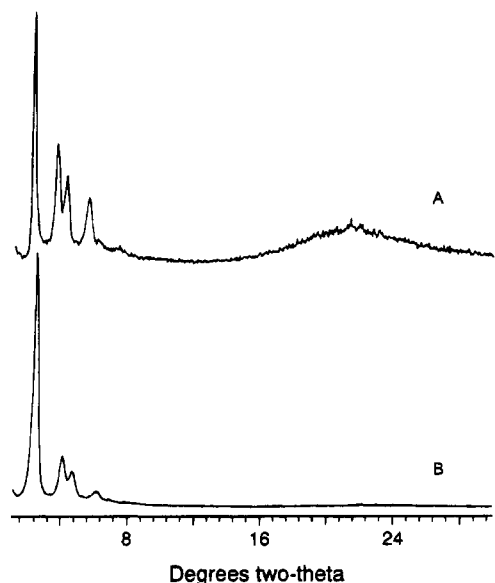


Figure 3. X-ray powder diffraction pattern of (A) CTMA MCM-41 formed from kanemite as-synthesized product and (B) calcined product.

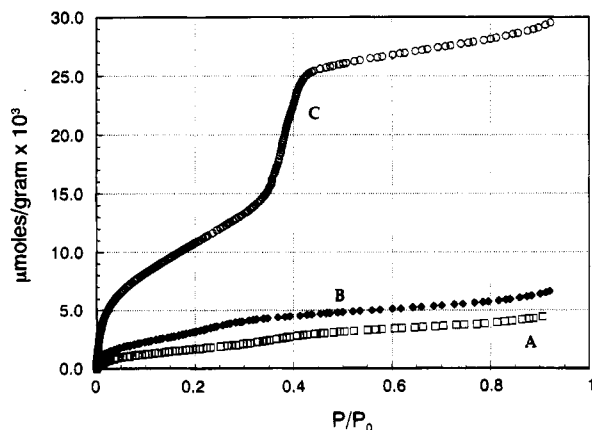


Figure 4. Argon isotherms of (A) calcined CTMA intercalated kanemite, (B) calcined DDTMA-intercalated kanemite, and (C) calcined MCM-41 samples.

CTMA intercalated kenyaite sample was first contacted TEOS and processed to the calcined product using the method describe by Landis et al.,⁸ the X-ray diffraction pattern exhibited broad peaks at approximately 40, 19, and 3.4 Å.

MCM-41 was prepared by combining 5 g of hydrated kanemite with 100 g of a 29 wt % (this is approximately 1 M) $C_{16}H_{33}(CH_3)_3N^+ OH/Cl^-$ solution with stirring. This mixture was placed in a polypropylene bottle and put into a steam box (100 °C) for 48 h. The resultant product was a clear solution indicating that the layered silicate reagent was completely dissolved. This solution was then titrated with conc. H_2SO_4 to reduce the pH from approximately 12.4 to 9.5 (this required 1.8 g of acid). A precipitate formed upon titration. The titrated mixture was returned to the steam box for 48 h. The final product was recovered by filtration, dried in air at ambient temperature, and calcined in air at 540 °C for 6 h. The X-ray diffraction patterns of the intermediate and the calcined material are shown in Figure 3a and b, respectively. Found in the final as-synthesized product (wt %): C, 36.8; N, 2.37; Si, 18.2; ash (1000 °C), 46.4.

Argon physisorption data for the calcined CTMA and DDTMA intercalated kanemite samples, the CTMA/silica intercalated kenyaite sample, and of MCM-41 are shown in Figures 4–6. Benzene sorption data for the calcined CTMA and DDTMA intercalated kanemite and MCM-41 samples are shown in Figure 7. Transmission electron microscopy data are illustrated in Figures 8 and 9 for the CTMA intercalated

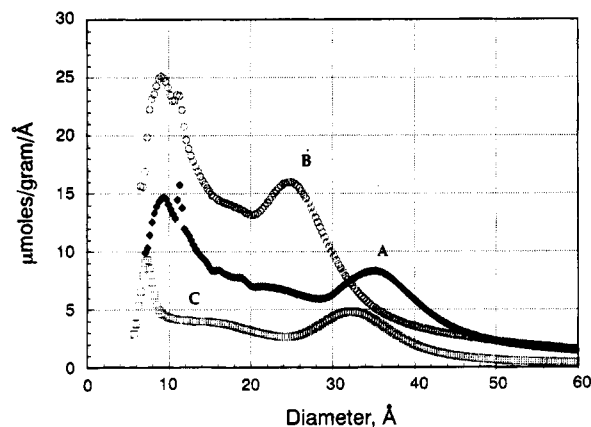


Figure 5. Horváth-Kawazoe plots of (A) calcined CTMA intercalated kanemite, (B) DDTMA intercalated kanemite, and (C) calcined CTMA/silica intercalated kenyaite.

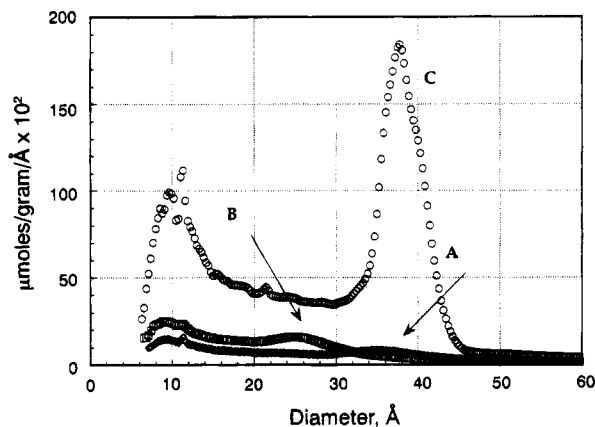


Figure 6. Horváth-Kawazoe plots of (A) calcined CTMA intercalated kanemite, (B) DDTMA intercalated kanemite, and (C) MCM-41 sample.

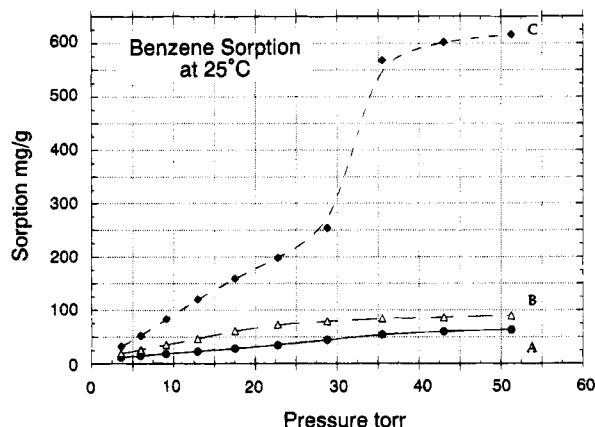


Figure 7. Benzene data of (A) calcined CTMA intercalated kanemite, (B) DDTMA-intercalated kanemite, and (C) calcined MCM-41 samples.

kanemite sample, Figure 10 for the DDTMA intercalated kanemite, and Figure 11 for the MCM-41 sample.

Rheological Analyses of Surfactant Solutions. The rheological data on a series of surfactant solutions were obtained using a cuvette geometry with a titanium bob and stainless steel cup. A dynamic strain sweep (0–50%) at 10 rad/s was conducted on four $C_{16}H_{33}(CH_3)_3N^+ OH/Cl^-$ solutions (at approximately 30, 3, 0.3, and 0.03 wt %) and four CTMA/Cl solutions (at approximately 30, 3, 0.3, and 0.03 wt %) at two temperatures, 20 and 65 °C. To eliminate any solution volatility, silicone oil, which was immiscible with the surfactant solutions, was used to cover the surface of the water/surfactant solution. The results are presented in Figure 12.

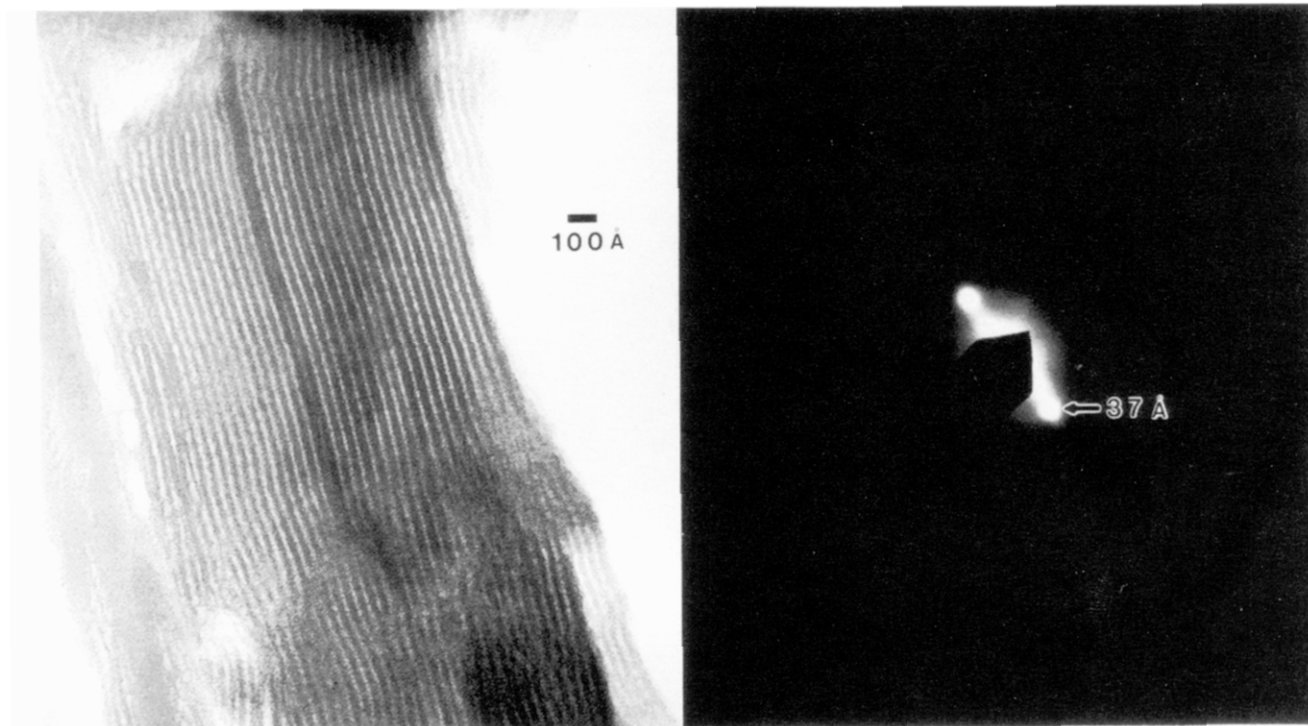


Figure 8. Transmission electron micrograph (left) and selected area electron diffraction pattern (right) from calcined CTMA intercalated kanemite.

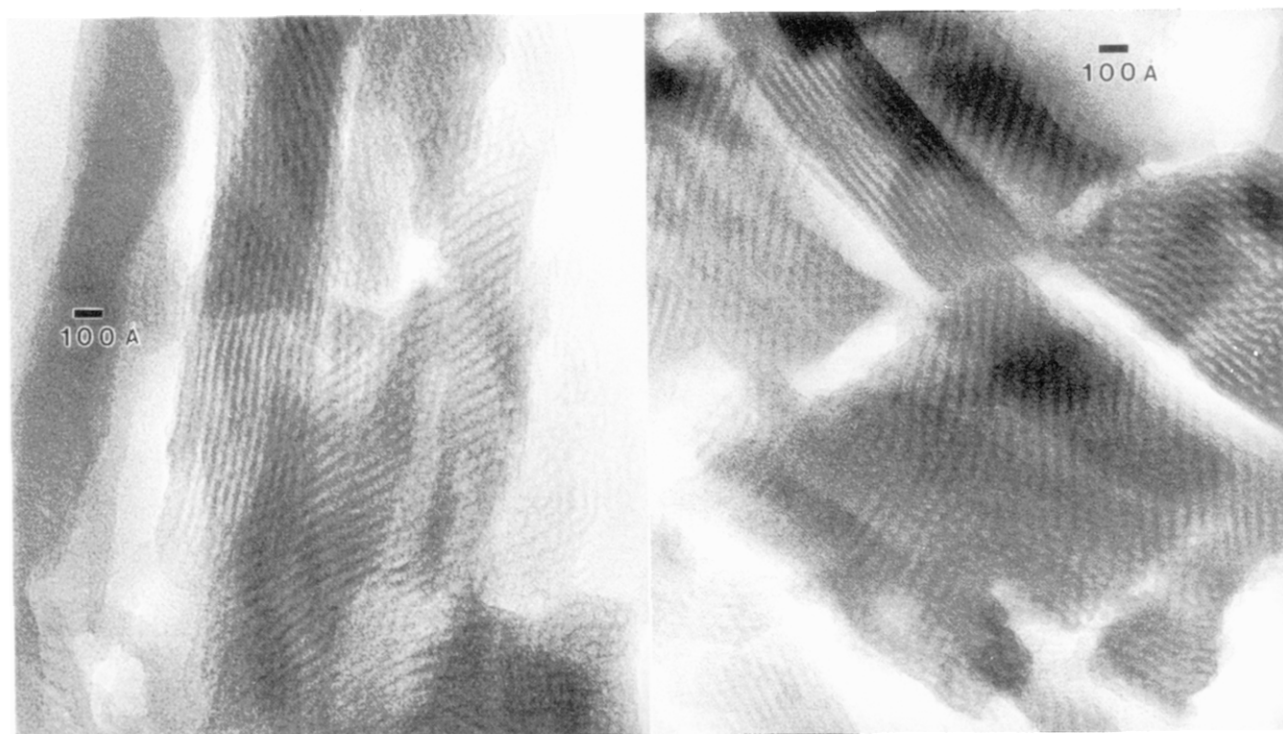


Figure 9. Transmission electron micrographs from calcined CTMA intercalated kanemite showing a variety of fringe patterns.

Results and Discussion

Intercalated Kanemite Materials. The X-ray diffraction patterns of the CTMA intercalated kanemite intermediates (Figure 1a and b) revealed several intense peaks having d spacings of approximately 37, 18, 12, and 4 Å for the first week sample and 38, 19, 13, and 4 Å for the second week sample. The X-ray patterns represent a series of low-angle peaks that are order reflections of the first peak and the retention of the most intense peak of the layered silicate reagent at 4 Å. The

X-ray diffraction patterns of both these intermediates suggest that the original layered structure of the layered silicate has been intercalated by the quaternary reagent. The X-ray diffraction pattern of the calcined product (Figure 1c) exhibited a relatively broad peak with a maxima at a d spacing of approximately 38 Å and an intense sharp peak at approximately 4 Å, indicating the retention of the original silicate layered structure.

The X-ray diffraction patterns (Figure 2a and b) of the DDTMA intercalated layered kanemite intermedi-

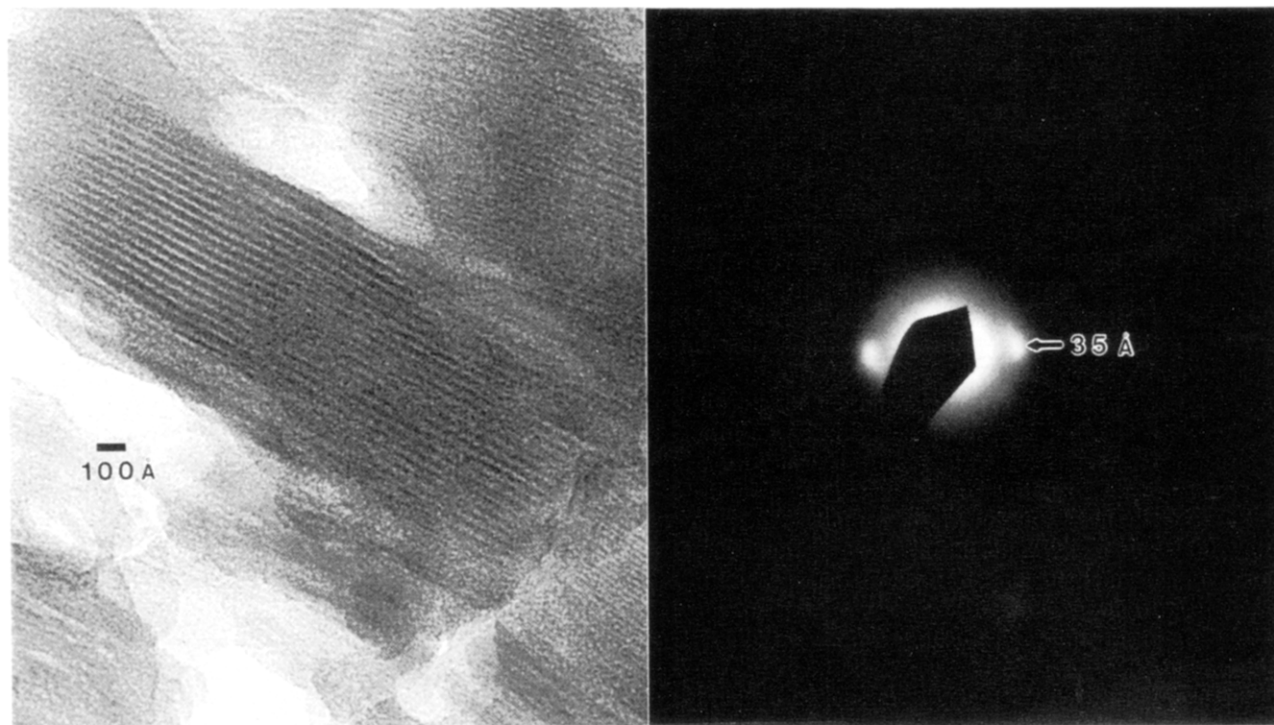


Figure 10. Transmission electron micrograph (left) and selected area electron diffraction pattern (right) from calcined DDTMA-intercalated kanemite.

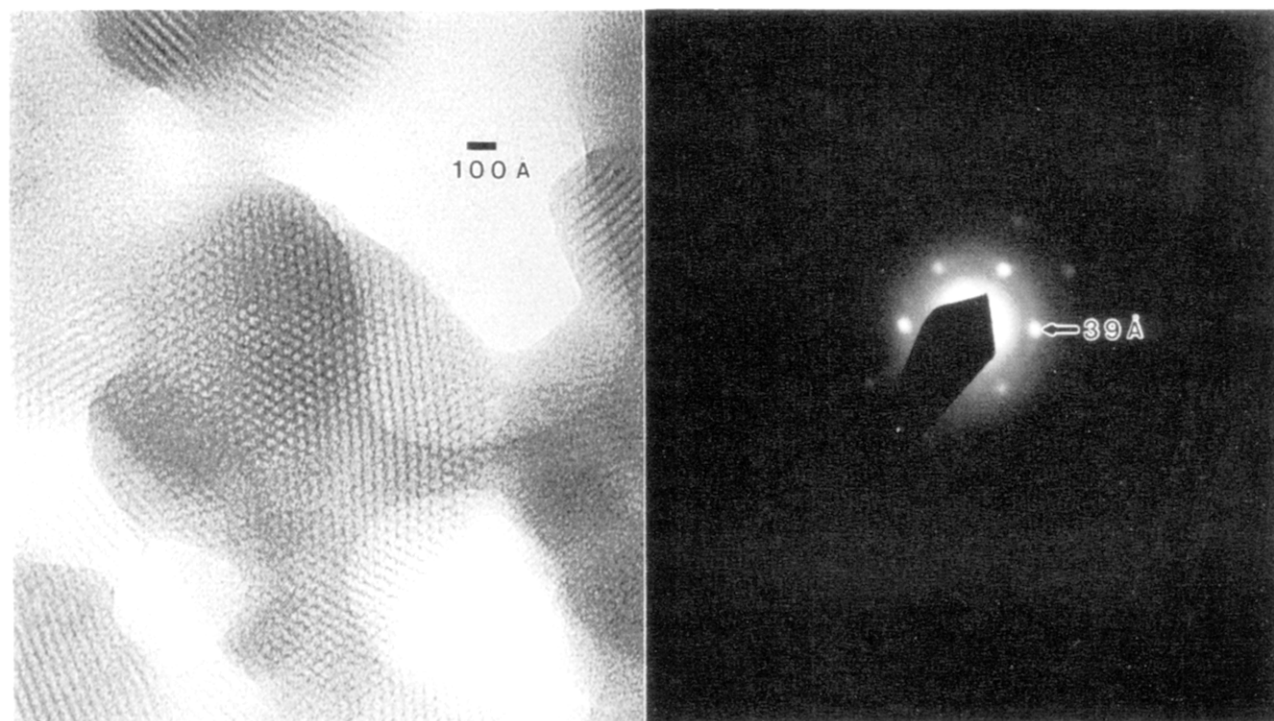


Figure 11. Transmission electron micrograph (left) and selected area electron diffraction pattern (right) establishing the presence of calcined MCM-41.

ates revealed several intense peaks having d spacings of approximately 34, 17, 12, and 4 Å for both the first-week sample and the second-week sample. These patterns also suggest an intercalated layered material having retained the silicate layered structure consistent with the CTMA derived sample described above. The X-ray diffraction pattern of the calcined product (Figure 2c) exhibited a relatively broad peak with a maximum at a d spacing of approximately 37 Å and an intense sharp peak at approximately 4 Å, again consistent with retention of the silicate layered structure.

The chemical analyses of the intercalated samples suggest that the surfactant molecules remain intact in the products. The C/N ratio for the CTMA derived material was 24 compared to an expected value of 19. For the DDTMA prepared material, the C/N ratio was 15 (one week) and 19 (final) compared to the expected value of 15. The N/Si ratio of these intercalated products was approximately 0.10.

Argon isotherms of the two calcined kanemite samples indicate rather broad pore size distribution, 30–40 and 20–30 Å (at half-peak width), and low pore volumes,

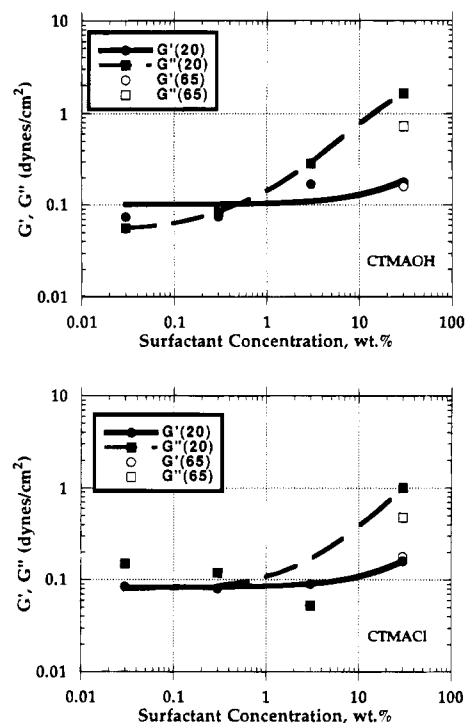


Figure 12. Rheological data of (top) 29 wt % $C_{16}H_{33}(CH_3)_3N^+OH/Cl^-$ solutions and (bottom) CTMACl solutions at various concentrations and at both 20 and 65 °C.

0.095 and 0.13 cm^3/g , respectively, for the CTMA and DDTMA intercalated products (Figures 4 and 5). Benzene sorption capacity at 25 °C for the two calcined kanemite derived samples are illustrated in Figure 7. For the CTMA intercalated sample the capacity was approximately 75 cm^3/g . The benzene sorption capacity for the DDTMA intercalated sample was approximately 110 cm^3/g .

Figure 8 is a typical electron micrograph and selected area electron diffraction pattern from a thin section of a CTMA-intercalated kanemite sample. The image shows an extensive area of expanded layers viewed edge-on, with an ≈ 40 Å repeat distance normal to the layers. The electron diffraction pattern is one-dimensional with a 37 Å primary repeat and some streaking along the central lattice line. Occasionally, images of I were obtained with fringe patterns more complex than those in Figure 8. Figure 9 shows two such electron micrographs. The features observed in these images may result from overlap of swollen/intercalated layered crystallites viewed edge-on but in differing orientations. Superposition of misoriented one-dimensional fringe patterns can produce (in projection) an illusion of a two-dimensional order. This is a likely explanation for features such as A and B in Figure 9 because some one-dimensional fringe patterns can be traced to regions where they appear to be two-dimensional, as would be the case if only part of the edge-on layered crystallite overlaid an underlying crystal in a different orientation. Other features such as C are more complex. This feature may be overlapping misoriented layers viewed edge-on wherein some of the layers are curved and bent. Alternatively, this region may represent a material with order in more than one dimension.

Figure 10 is a typical electron micrograph and selected area electron diffraction pattern from a thin section of the DDTMA-intercalated kanemite sample.

The image shows an extensive area of expanded layers viewed edge-on, with an ≈ 35 Å repeat distance normal to the layers. The electron diffraction pattern has maxima at the ≈ 35 Å repeat distance.

The X-ray diffraction patterns of the calcined CTMA intercalated kenyaite exhibited a broad peak at approximately 3.5 Å, suggesting retention of the silicate layered structure. However, there were no retention of any low-angle peaks suggesting collapse of the silicate layers upon the removal of the surfactant molecules. When the CTMA intercalated sample was treated with TEOS prior to calcination, the X-ray diffraction pattern of this material exhibited a low-angle peak indicative of some degree of layer separation. The argon physisorption data (Figure 5) indicates a broad pore size distribution, 26–36 Å, similar to that of the CTMA-intercalated silicate discussed above. The calculated pore volume of the intercalated kenyaite sample is 0.11 cm^3/g , similar to that of the intercalated kanemite samples discussed previously.

The absence of any stable mesoporous silicate formed from the CTMA/kenyaite preparation similar to that of the CTMA/kanemite system suggests a difference in reactivity of these two layered silicates. The variation in the thickness of the silicate layers of these materials may be a factor in the ability to intercalate these two layered materials. Kanemite is reported to consist of silicate layers of approximately 4 Å, whereas the silicate layers of kenyaite are approximately 12 Å thick.^{4,7}

MCM-41. The X-ray diffraction patterns of the MCM-41 intermediate (Figure 3a) revealed several intense peaks having d spacings of approximately 41, 25, 21, and 16 Å which can be indexed for $hk0$ reflections of a hexagonal unit cell. There were no peaks located at approximately 4 Å characteristic of the layer structure of the reactant silicate. The X-ray diffraction pattern of this calcined MCM-41 sample (Figure 3b) displayed intense peaks having d spacings at approximately 38, 22, 19, and 15 Å. This pattern illustrates the lattice contraction of approximately 3 Å and the retention of the hexagonal $hk0$ indexing of MCM-41 upon calcination, both characteristics of MCM-41 materials.²

The chemical analyses of the MCM-41 product also suggest retention of the surfactant. The C/N ratio was 18 compared to the expected value of 19. The N/Si ratio of the MCM-41 material was 0.26, about 150% higher than those of the intercalated silicate samples suggesting a larger interaction of the organic in the formation of MCM-41.

The argon sorption isotherms of MCM-41 and the intercalated materials are compared in Figure 4. MCM-41 shows a very sharp inflection point at $\sim 0.35 P/P_0$ indicating capillary condensation within a uniform pore size (approximately 38 Å).^{6,9} The MCM-41 sample has significantly higher pore volume, 0.74 cm^3/g , and a narrow pore size distribution, 6 Å (at half-peak width), relative to the intercalated silicate materials (Figure 6). The Horváth–Kawazoe plot indicates a narrow pore size distribution for MCM-41 similar to those of molecular sieves.

(7) Beneke, K.; Lagaly, G. *Am. Mineral.* **1983**, *68*, 818–26.

(8) Landis, M. E.; Aufdembrink, B. A.; Chu, P.; Johnson, I. D.; Kirker, G. W.; Rubin, M. K. *J. Am. Chem. Soc.* **1991**, *113*, 3189–90.

(9) Gregg, S. J.; Sing, K. S. W. *Adsorption, Surface Area, and Porosity*, 2nd ed.; Academic Press: New York, 1982.

The benzene sorption capacity of the MCM-41 sample is shown in Figure 7. The total capacity was approximately 750 cm³/g, and the data exhibit a sharp inflection characteristic of capillary condensation within uniform pores, where the p/p_0 position of the inflection point (~ 30 Torr) is related to the diameter of the pore. These data suggest a uniform pore size which is also shown in the argon physisorption analysis of the MCM-41 sample.

Figure 11 shows a typical electron micrograph and a selected area electron diffraction pattern from a thin section of the MCM-41 sample. In contrast to the previous samples, this specimen contains regions of well-formed large-pore material with apparent hexagonal symmetry, as can be seen in the image in Figure 11. The associated electron diffraction pattern shows the $\{1,0,-1,0\}$ family of reflections with a $d_{100} = 39$ Å. These results indicate the presence of MCM-41 in the sample.

Rheological Analyses. Two stress coefficients that give information on the system studied are the storage modulus, G' , and the loss modulus, G'' . These moduli provide information about the structure of the material being measured. In Figure 12, for both 29 wt % CTMACl and 29 wt % C₁₆H₃₃(CH₃)₃N⁺ OH/Cl⁻ solutions, G' and G'' start to increase for surfactant concentrations between approximately 3 and 30 wt %. Similar concentration dependence of G' and G'' has been obtained by Hoffmann et al.^{10,11} in surfactant solutions such as cetylpyridinium salicylate, alkylpyridinium salicylate, and alkyltrimethylammonium salicylate. According to Hoffmann et al.^{12,13} and Davis,¹⁴ surfactant micellar structure changes from spherical to rod as the concentration of surfactant increases. Luzzati¹⁵ and Tiddy¹⁶ have used small-angle X-ray scattering techniques on many surfactant systems, including CTMACl. For CTMACl solutions the transformation from individual molecules to spherical micelles occurs at surfactant concentrations of <4.5 wt % and the transformation to a liquid-crystal phase (middle) occurs at ~ 40 wt %. Their data would suggest that the changes in G' and G'' values for the surfactant solutions, illustrated in Figure 12, may be the appearance of the surfactant micelles necessary for M41S formation. This transformation to micellar species takes place at room temperature at a surfactant concentration between 3 and 30%. As concentration increases, both CTMACl and 29 wt % C₁₆H₃₃(CH₃)₃N⁺ OH/Cl⁻ surfactant solutions generate this surfactant structure; the solution with 29 wt % C₁₆H₃₃(CH₃)₃N⁺ OH/Cl⁻ solution has more structure than the corresponding CTMACl containing solution; also from Figure 12, we can see that increases in G' and G'' at 65 °C are less than those at 20 °C, which means that there is more structure at 20 °C. In fact, all of the

data at 65 °C for solutions less than 30% are below the detection limit of the spectrometer. The higher thermal activity of the solution and surfactant solubility at 65 °C may explain this behavior. Both conditions should reduce the possibility of micellar formation. Similar observations have been reported in other surfactant solutions.^{17,18}

Mechanism of Formation. A templating mechanism (liquid-crystal templating, LCT) in which surfactant liquid-crystal structures serve as organic templates has been proposed for the formation of M41S type materials.^{1,2} The generation of varied pore size MCM-41 either by use of different length surfactant molecules or by use of auxiliary organics¹ and the existence of M41S materials having structures (hexagonal, cubic, and lamellar)^{2,19} that mimic known liquid-crystal phases are strong evidence to support this mechanism. Proposed mechanism pathways suggest either (A) the presence of the liquid-crystal phase prior to the addition of the reagents or (B) that the silicate species generated in the reaction mixture influences the ordering of surfactant micelles to the desired liquid-crystal phase.²

For either pathway, the resultant composition produces an inorganic material that mimics known liquid-crystal phases. For pathway A to be operative, it is required that the surfactant molecules exist in sufficient concentration for the liquid crystal to form. This liquid-crystal structure serves as the templating agent, and the inorganic silicate anions merely serve to counterbalance the charge of these fully ordered surfactant aggregates. Literature data suggest that for the cetyltrimethylammonium cation system, at the concentrations used to form M41S structures, the presence of the various liquid-crystal structures appears unlikely. Our room-temperature rheology data indicate that the surfactant concentration has to be greater than about 3% for any structure to be detected. This molecular structure is presumably the transformation from the individual surfactant molecules to micelles not the formation of liquid crystal phases. At higher temperatures (65 °C) the formation of any structure is less likely, especially at surfactant concentrations less than 30%. Synthesis data also do not support pathway A. The ability to form the hexagonal, cubic, and lamellar M41S structures simply by varying the silica concentration at constant initial surfactant concentration is strong evidence against the requirement of a M41S template from a preexisting liquid-crystal phase.¹⁹

For pathway B, the presence of surfactant is only part of the template. The presence of a silicate anion species not only serves to charge balance the surfactant cations but also participates in the formation and ordering of the liquid-crystal phase. The exact nature of this organosilicate species is still uncertain. However, this organosilicate intermediate should be labile enough to form the various M41S structures. This intermediate must still retain sufficient surfactant (organic) character to form liquid-crystal phases. The formation of liquid-

(10) Hoffmann, H.; Rehage, H.; Reizlein, K.; Thurn, H. *Macro- and Microemulsions Theory and Applications*; ACS Symposium Series No. 272; Shah, D. O., Ed.; American Chemical Society: Washington, DC, 1985; pp 41–66.

(11) Kalus, J.; Hoffmann, H. *J. Chem. Phys.* **1987**, *87*, 714–22.

(12) Hoffmann, H.; Platz, G.; Rehage, H.; Schorr, W. *Ber. Bunsenges. Phys. Chem.* **1981**, *85*, 877–82.

(13) Hoffmann, H.; Platz, G.; Rehage, H.; Schorr, W. *Adv. Colloid Interface Sci.* **1982**, *17*, 275.

(14) Davis, H. T. *Adv. Chem. Eng.* **1991**, *16*, 169–89.

(15) Reiss-Husson, F.; Luzzati, V. *J. Phys. Chem.* **1964**, *68*, 3504–11.

(16) Henriksson, U.; Blackmore, E. S.; Tiddy, G. J. T.; Soderman, O. *J. Phys. Chem.* **1992**, *96*, 3894–3902.

(17) Hoffmann, H.; Rehage, H.; Schorr, W.; Thurn, H. *Surfactants in Solutions*; Mittal, K. L., Lindman, B., Eds.; Plenum Press: New York, 1984; Vol. 1, pp 425–54.

(18) Hoffmann, H.; Rehage, G.; Platz, G.; Schorr, W.; Thurn, H.; Ulbricht, W. *Colloid Polym. Sci.* **1982**, *260*, 1042–56.

(19) Vartuli, J. C.; Schmitt, K. D.; Kresge, C. T.; Roth, W. J.; Leonowicz, M. E.; McCullen, S. B.; Hellring, S. D.; Beck, J. S.; Schlenker, J. L.; Olson, D. H.; Sheppard, E. W., submitted for publication.

crystal phases from an intermediate having predominantly silica (inorganic) character, such as crystalline layered structure, appears less likely.

Neither LCT mechanism pathway proposes a layered intermediate for the formation of these mesoporous molecular sieves. The absence of any X-ray diffraction evidence for the existence of a well-defined crystalline layered structure supports this exclusion. The formation of the intercalated silicate materials appears to take place with retention of this crystalline silicate layered structure. The X-ray diffraction patterns of the intermediates as well as the final calcined products contained the characteristic peak associated with the single silicate layer. MCM-41 was observed only when the layered silicate material was dissolved and combined with sufficient surfactant solution. In this experiment the layered material served as a source of silica similar to those cited in the literature.² There was sufficient base present to solubilize the silicate reagent. X-ray diffraction patterns of the intermediate and the final calcined product of the MCM-41 material represent a material formed having a hexagonal array of pores, not one formed from a layered material. This method of using a layered silicate as a silica source for the formation of MCM-41 appears to be supported by some recent work by Inagaki et al.²⁰ These researchers obtained MCM-41 from a kanemite/CTMACl system by first heating the mixture to 70 °C for 3 h followed by titration of the silicate containing suspension to a pH of 8.5. X-ray diffraction data and transmission electron micrographs suggest that a material similar to MCM-41 formed. The absence of any peaks having a d-spacing of approximately 4 Å in the X-ray diffraction pattern of the "MCM-41-like" material also suggests that the layered structure of kanemite no longer exists. Their method of preparation and resultant product is similar to that of the MCM-41 preparation reported here.

Recently, Monnier et al.²¹ and Chen et al.²² have explored the details of the liquid-crystal templating mechanism we first proposed.^{1,2} These workers suggest that the precursor to the hexagonal member of the M41S family is either an ion-pair complex of the silicate oligomers and surfactant molecules²¹ or a collection of individually silicated surfactant rods.²² In both of these proposed mechanisms, the intermediates are silicate

clad structures which are consistent with the proposed silicate initiated pathway. Monnier et al. have proposed that the transformation from this silicate-surfactant complex precursor to the hexagonal MCM-41 structure appears to involve essentially bilayers of silicate/surfactant species rather than some well-defined crystalline silicate layer.²¹

Conclusion

The formation mechanisms for MCM-41 and the layered silicate derived mesoporous materials are different. MCM-41 is formed from a silicate anion initiated liquid-crystal templating mechanism. The formation of M41S materials such as MCM-41 (hexagonal), MCM-48 (cubic), and the lamellar material that mimic known liquid-crystal phases supports this proposed mechanistic pathway. The layered silicate derived materials appear to form by the intercalation of the layered silicate using the surfactant present in the synthesis mixture. Retention of the silicate layer throughout the formation process supports the intercalation mechanism. Rheological data of the surfactant solutions used to form both of these porous materials also support the different mechanism pathways. For the more concentrated solutions typically used in MCM-41 synthesis, the data suggest the presence of micellar structure, whereas in the lower surfactant concentration used in the intercalation synthesis system there was no evidence for solution structure. Only when layered silicate structure is destroyed by dissolution does it serve as a silica source for the formation of MCM-41. Although layered silicate based materials have mesopores of similar size as MCM-41 products, the pore size distribution is broader, similar to that of a layered product. MCM-41 materials also have 5 times the total pore volume and hydrocarbon sorption capacity compared to the layered silicate derived materials.

Acknowledgment. The authors are grateful to the staff at Mobil's Central and Paulsboro Research Laboratories for their invaluable discussion and effort. In particular, we acknowledge C. D. Chang, R. M. Dessau, and H. M. Princen for alerting us to references in the surfactant literature and helpful discussions on surfactant liquid-crystal phases. We thank N. H. Goeke, K. A. German, and D. F. Colmyer for their expert technical assistance and W. J. Roth, J. S. Beck, K. D. Schmitt, D. H. Olson, and J. B. Higgins for helpful technical discussions. We also thank Mobil Research and Development Corp. for its support.

(20) Inagaki, S.; Fukushima, Y.; Kuroda, K. *J. Chem. Soc., Chem. Commun.* **1993**, 8, 680-82.

(21) Monnier, A.; Schüth, F.; Huo, Q.; Kumar, D.; Margolese, D.; Maxwell, R. S.; Stucky, G. D.; Kishnamurthy, M.; Petroff, P.; Firouzi, A.; Janicke, M.; Chmelka, B. F. *Science* **1993**, *261*, 1299-1303. Alfredsson, V.; Keung, M.; Monnier, A.; Stucky, G. D.; Unger, K. K.; Schüth, F. *J. Chem. Soc., Chem. Commun.* **1994**, 921-22.

(22) Chen, C. Y.; Burkett, S. L.; Li, H. X.; Davis, M. E. *Microporous Mater.* **1993**, *2*, 27-34.